4th International Conference on
Earthquake Geotechnical Engineering
June 25-28, 2007
Paper No. 1611

GROUND MOTION AMPLIFICATION IN SAN GIULIANO DI PUGLIA (SOUTHERN ITALY) DURING THE 2002 MOLISE EARTHQUAKES

Rodolfo PUGLIA[1], Giuseppe LANZO[2], Alessandro PAGLIAROLI[3], Stefania SICA[4], Francesco SILVESTRI[5]

ABSTRACT

On October 31, 2002, a M_L=5.5 earthquake struck the Molise region in Southern Italy. The strongly non-uniform damage distribution observed in the town of San Giuliano di Puglia suggested that site amplification significantly affected the seismic response of the area. Soon after the earthquake, a seismic microzonation study was undertaken on the basis of a detailed geotechnical investigation of the subsoil, including field and laboratory standard and advanced tests. The main geotechnical formations identified in the area consisted of a soft rock formation (flysch) and a deep layer of marly clays. Several aftershocks were recorded by two temporary accelerometric stations located in the ancient and recent zones of the town, on the flysch outcrop and the fine-grained soil respectively. The field and laboratory experimental data allowed the definition of the geotechnical model of the subsoil. The analysis of a deep electric tomography and the frequency content of the aftershocks indicated a thickness of about 300 m for the marly clay formation beneath the accelerometric station in the recent part of the town, but a full description of the bedrock geometry has been not yet achieved. To envisage a more reliable definition of the subsoil model, the results of 2D seismic response analyses carried out referring to different hypotheses were compared to the peak amplitudes and frequency contents recorded during the aftershocks.

Keywords: Site amplification; Flysch; Marly clays; Aftershocks recordings; Numerical analysis.

INTRODUCTION

On October 31, 2002, a M_L=5.5 earthquake struck the Molise region in Southern Italy (Fig. 1). The earthquake was followed by a comparable aftershock (M_L=5.4) nearby on the day after, and by a series of seismic events of lower energy in the following month. In the town of San Giuliano di Puglia, located on the top of a ridge extending about 1 km along the NNW-SSE direction (Fig. 2a), the distribution of the damage consequent to the mainshocks was strongly non-uniform: the old part, which was less damaged, lies on outcropping rock, while the most severe damages were surprisingly concentrated in the new part of the town, lying on fine-grained soils. Such evidence suggested that differential site amplification significantly affected the seismic response in the town. The hypothesis was confirmed by aftershock records (Table 1) logged by two temporary accelerometric stations (Fig. 2a,c), located in the ancient (close to a church) and in the new portions of the town (close to a school which collapsed during the main event), respectively.

[1] PhD Student, DDS, University of Calabria, Italy. Email: RPuglia@dds.unical.it
[2] Professor, DISG, University of Rome “La Sapienza”, Italy. Email: giuseppe.lanzo@uniroma1.it
[3] Research Assistant, DISG, University of Rome “La Sapienza”, Italy.
Email: alessandro.pagliaroli@uniroma1.it
[4] Research Associate, Department of Engineering, University of Sannio, Italy.
Email: stefsica@unisannio.it
[5] Professor, DDS, University of Calabria, Italy. Email: f.silvestri@unical.it

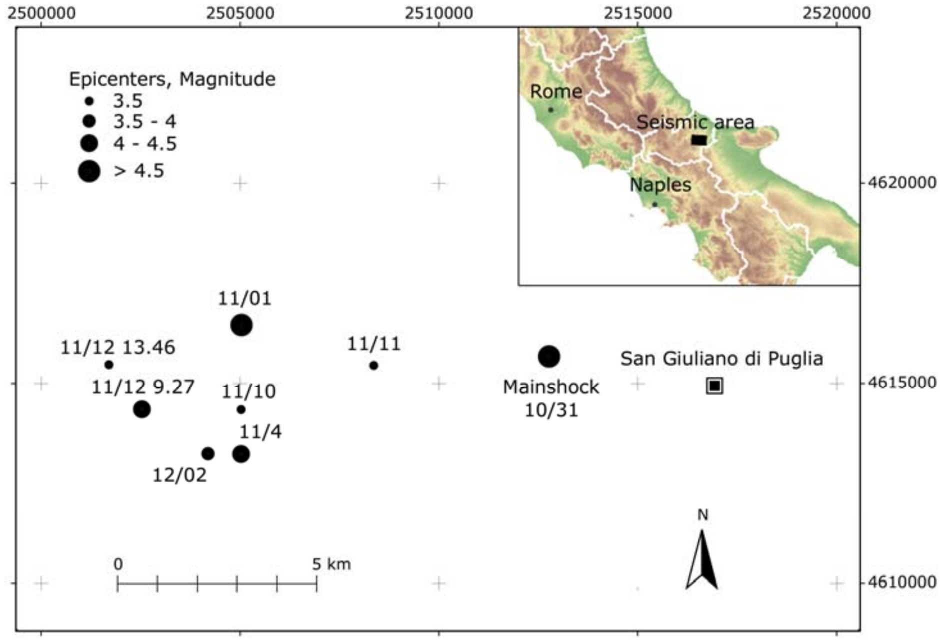

Figure 1. Epicenters and magnitudes of the 2002 Molise earthquakes (after Silvestri et al., 2006)

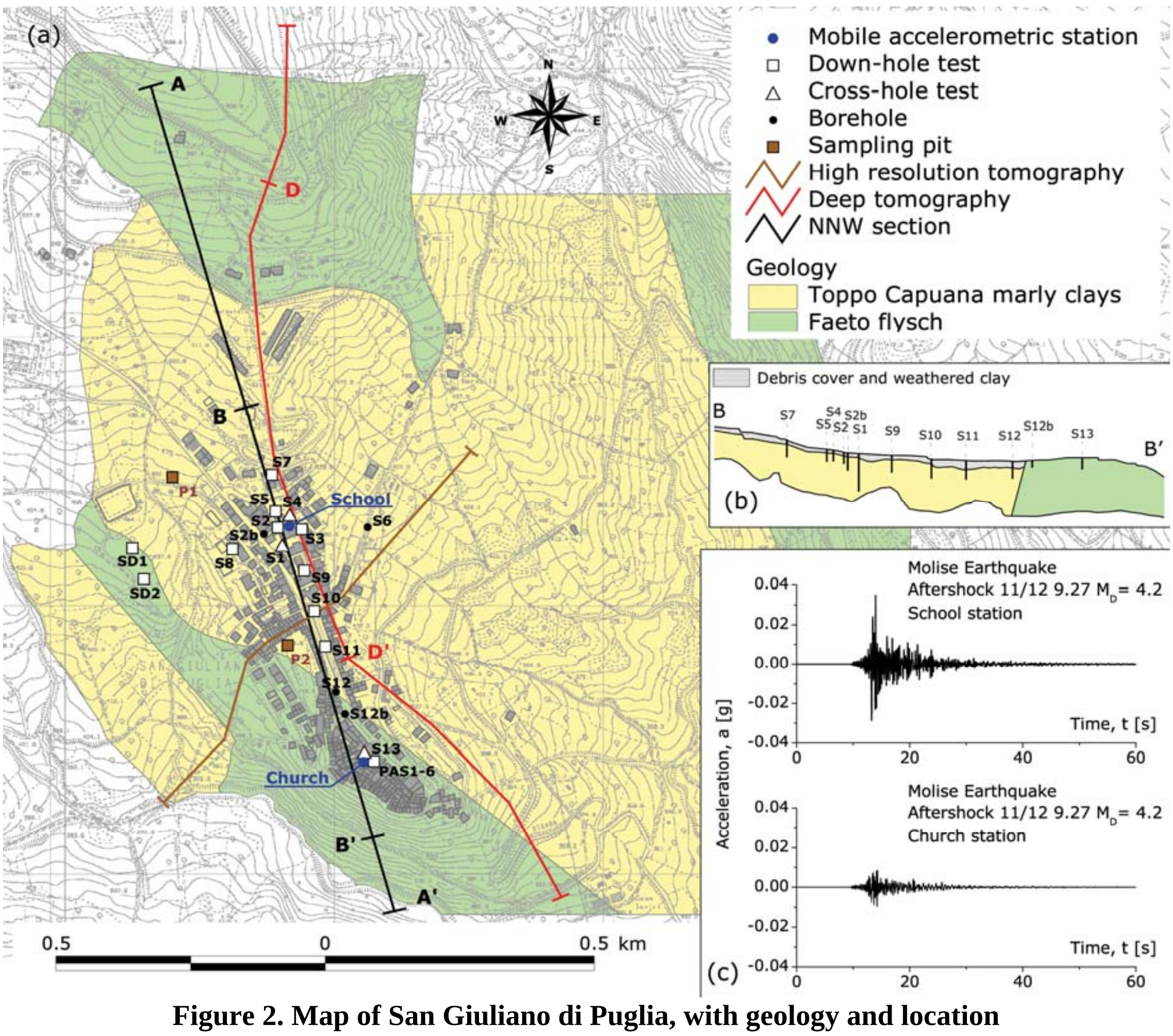

Figure 2. Map of San Giuliano di Puglia, with geology and location of main geotechnical and geophysical investigations (a); NNW section (b) with indication of the borehole depths; horizontal acceleration time histories (c) recorded at School and Church stations during 11/12 9.27 aftershock (after Silvestri et al., 2006b)

Table 1. Some aftershocks recorded by the mobile accelerometric stations

Id. code	Date	hh:mm	Lat	Lon	Depth [km]	M_L	M_W	PGA [g]	
								Church	School
026	11/10	12:23	41.682	14.846	12.94	3.6		0.0027	0.0067
028	11/11	18:32	41.701	14.863	17.80	3.5		0.0023	0.0091
030	11/12	09:27	41.703	14.800	17.50		4.2	0.0088	0.0345
031	11/12	13:46	41.693	14.794	16.10		3.6	0.0010	0.0047
040	12/02	20:52	41.680	14.886	3.96	4.0		0.0038	0.0094

This paper summarises the results of the geotechnical investigation used to define different subsoil models for the seismic response analyses, which were calibrated and compared on the basis of the aftershocks recordings, as described in the following pages.

SUBSOIL INVESTIGATION AND MODELLING

In order to develop a seismic microzonation of the area, the *Department of Civil Protection* (DPC) of the Italian Government committed a comprehensive study on the subsoil properties to different companies and university laboratories (Baranello et al., 2003). The knowledge on subsoil properties was later integrated by further investigations for the reconstruction of the town centre, and by geophysical surveys carried out in the framework of the *INGV-S3 Project*, again funded by DPC.

The field investigation included a large number of boreholes, sampling pits, in situ piezometric measurements, CPT, SCPT, cross-hole (CH) and down-hole (DH) tests. The laboratory experimental programme involved oedometer, triaxial and cyclic/dynamic torsional shear tests on undisturbed samples of fine-grained soils, analysed in detail by Silvestri et al. (2006a). The results relevant for the subsoil modelling are described in the comprehensive report by Silvestri et al. (2006b).

Geological settings and deep geophysical surveys

On the basis of surface surveys and through the analysis of borehole logs (some of which shown in Fig.2a), most geological studies (e.g. Baranello et al., 2003; Melidoro, 2004; Giaccio et al., 2004; Guerricchio, 2005) agree to recognise that the main formations present at San Giuliano di Puglia are: the ‘Faeto flysch’ (FF), that is a sedimentary succession of calcareous, arenaceous and marly soils, either coarse or fine-grained; a deep deposit of Toppo Capuana marly clays (MC), weathered down to few metres, and covered by a shallow layer of disturbed soil and landslide debris.

In the Southern part of the town the clayey formation is in lateral contact with the outcropping flysch, which there appears to be intact, and constitutes the foundation soil of the less damaged historical buildings (B-B’ section in Fig. 2b). In the Northern part of the ridge, the flysch is heavily tectonised and fractured, and the contact with the marly clays is of uncertain geometry. Baranello et al. (2003) suggested that the shape of the clay deposit could be that of a basin, resulting from a synclinal deformation of the flysch structure (Fig. 3a). A second hypothesis (Giaccio et al., 2004) assumes that the contact results from the thrusting and oversliding of the flysch against and above the clays, and that therefore the clay deposit might assume a ‘wedge’ shape such as that sketched in Fig.3b.

Three geo-electric resistivity tomographies (ERT) carried out in 2005 for the S3 Project across two NNW-SSE and one NE-SW sections did not clarify completely the nature and the geometry of the flysch-clay stratigraphic contact (Silvestri et al., 2006b). However, the D-D’ section along the deep NNW-SSE tomography shown in Fig. 3 appears to describe an inclined contact between the flysch and the clays at the northern side of the ridge; it also individuates a limb of a stiff formation underlying the clay formation at a depth of about 300m. This latter finding was already suggested, as shown later, by the analysis of the frequency content of the aftershocks records (Petillo, 2004; Silvestri et al., 2006b), and has been recently confirmed by deep gravimetric profiling in the area (Palmieri et al., 2006).

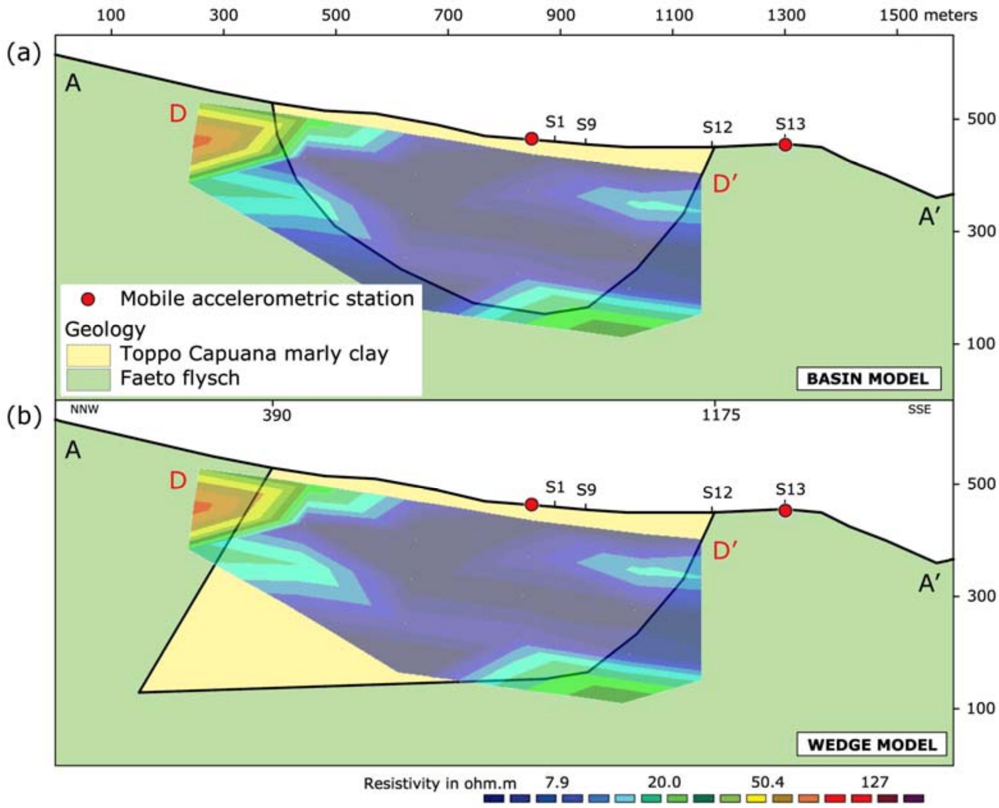

Figure 3. Working hypotheses for (a) basin and (b) wedge structures along NNW-SSE section with indication of soil resistivity from deep tomography

Geotechnical characterisation

In the seismic site response (SSR) analyses, the Faeto flysch was characterised as a linear visco-elastic material; only few among the several cross-hole (S13) and down-hole (SD1-2, PAS1-6) tests carried out during the different investigation stages permitted to obtain data on the shear wave velocity of the soft rock formation. Due to the low quality of CH test data[6] at S13, and to the large distance of the DH test sites SD1-2, the V_S profile assumed for the subsoil of the town centre was based on the data gathered from the DH PAS1-6, carried out up to 40 m, i.e. close to the location of the southern accelerometric station, which had been placed nearby to the old town church. The measurements shown in Fig. 4 with a dotted green line were averaged by a step profile, showing in the first 15m a gradual increase of V_S from 400 to 800 to 1350 m/s.

The results from laboratory and in situ tests were combined for the geotechnical modelling of the clayey marls. According to Melidoro (2004) and Guerricchio (2005), the Toppo Capuana formation consists of three principal units:

- a 'debris cover', of less than five metres thickness, including made ground, organic matter and shallow colluvial sediments;
- a layer, of two to ten metres thickness, of 'weathered tawny clays', characterised by medium to intense fissuring, resulting from the weathering and disturbance of the uppermost formation;
- a deep layer of Toppo Capuana marly clays, called 'grey clays', characterised by less intensely fissured meso-structure (Silvestri et al., 2006a).

The borehole seismic tests carried out in the verticals indicated in Fig. 2a were used as a primary reference for the analytical description of shear wave velocity profiles. The ranges of V_S obtained by

[6] The CH data have been shown to overestimate the measurements of V_S, because executed with a non-polarised source type ('sparker') which did not allow to clearly distinguish the arrival times of SV waves from those of the P waves. Therefore, only the DH data have been considered reliable for the subsoil modeling (Silvestri et al., 2006a,b).

DH tests are shown in Fig. 4 as average ± one standard deviation values; the data have been drawn with different colours according to the layering. The plot also shows the laboratory measurement of V_S from resonant column (RC) tests driven at consolidation stresses comparable with the in-situ effective overburden stress; it can be noted that for the tawny and grey clay, the laboratory data points tend to fall below the average V_S values from field DH measurements. This finding was attributed by sampling disturbance, re-consolidation procedure and variable degree of fissuring of the samples (see Silvestri et al., 2006a). In fact, as the fissuring spacing increases from tawny to grey clays, the scale effect for these latter seems to more sensibly affect the discrepancy between laboratory and field measurements.

The values of shear wave velocity measured at the end of the consolidation stages in RC tests on the tawny and grey clay samples were fitted by the power function:

$$V_S = A \cdot \left(p'\right)^b \tag{1}$$

where, expressing V_S in m/s and *p'* in kPa, *A*=162 and 202, and *b*=0.104 and 0.108, respectively for the tawny and grey clays. The resulting power law variations of V_S with depth are shown with dotted lines in Fig. 4. The $V_S(z)$ profile for the SSR analyses, drawn with a solid black line in Fig.4, was obtained by scaling the laboratory $V_S(z)$ relationships to the average field values (black dots in the same figure).

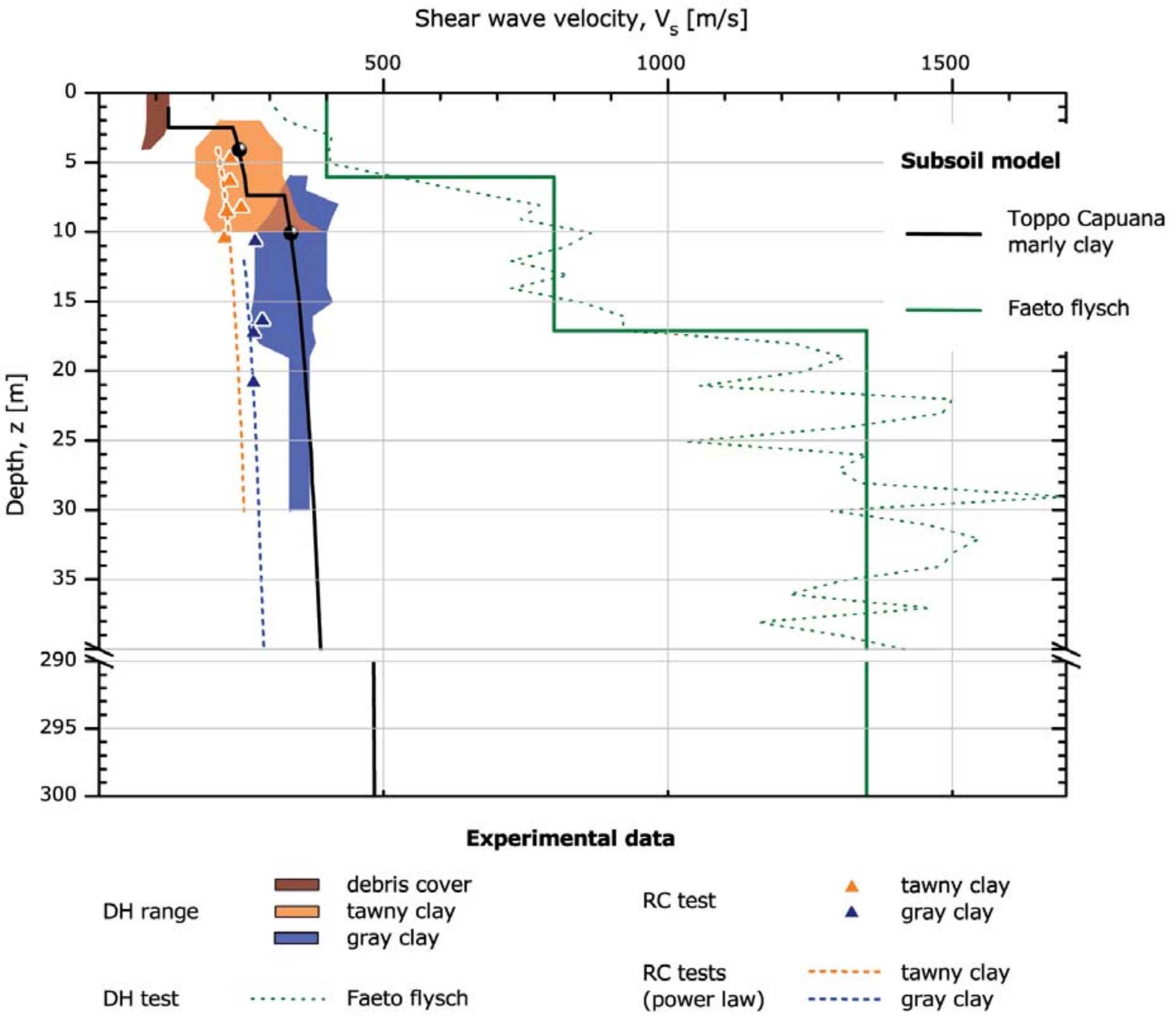

Figure 4. Shear wave velocity profiles in Toppo Capuana marly clays and Faeto flysch (modified after Silvestri et al., 2006b)

The non-linear pre-failure behaviour of the three units of the marly clay formation was analysed by means of RC test data at medium strain levels. Figure 5 shows the experimental results obtained for the different sets of samples in terms of normalised shear modulus, G/G_0 (upper plots), and damping ratio, D (lower plots), versus shear strain, γ. Since each set of experimental results showed comparable trends, they were interpreted using the Ramberg-Osgood (R-O) model, obtaining the analytical curves drawn in the plots. The difference in the decay curves of the three units are not very significant: it can be noted, however, that with the increase of depth of the layers, the linear strain range extends slightly and the decay of stiffness becomes sharper.

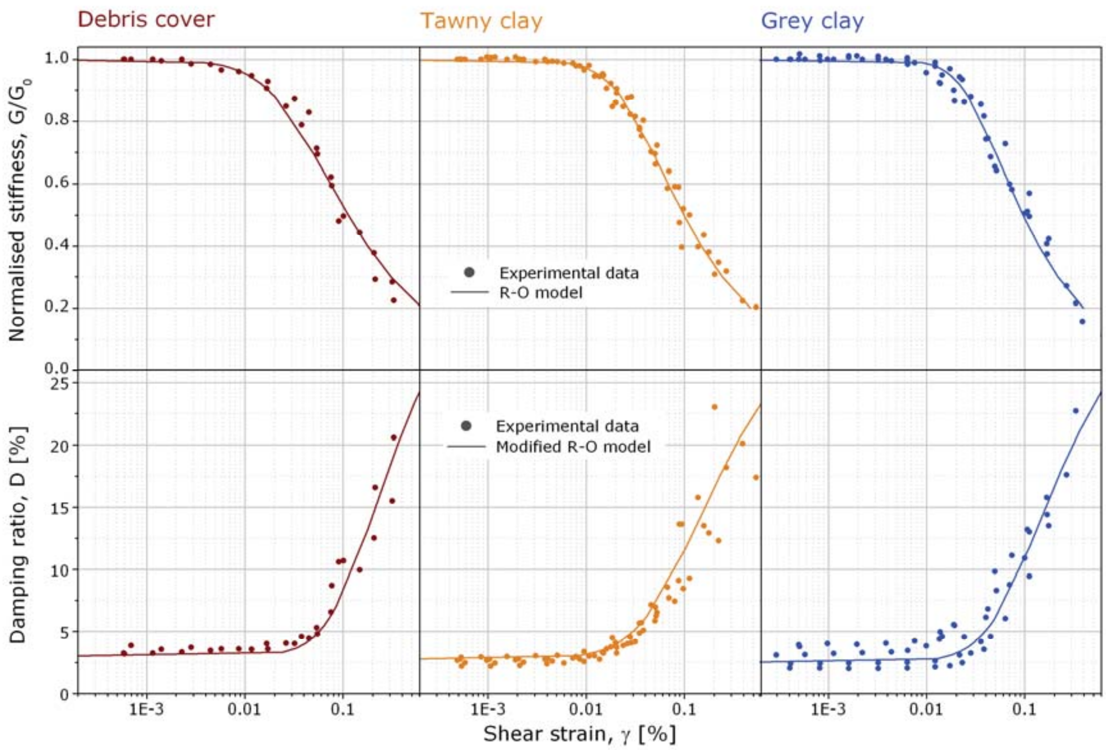

Figure 5. Variation of normalised shear modulus and damping ratio with shear strain for the three sub-units of the Toppo Capuana marly clays after RC tests (after Silvestri et al., 2006a)

GEOTECHNICAL MODELS FOR SITE RESPONSE ANALYSES

To assess the above described geological and geotechnical models, linear equivalent simulations of the aftershocks were carried out by 1D and 2D analyses.

In the preliminary research stage, 1D analyses solved in the frequency domain by the code EERA (Bardet et al., 2000), represented a valuable support to detect the "operative" bedrock depth, as previously anticipated. A 'back-analysis' of the unknown thickness of the grey clay was performed (Petillo, 2004), by varying its value from 75 to 500 m in a layered subsoil model, corresponding to the vertical S1, close to the northern seismic station (see Figs. 2-3). Comparing the first seven computed natural frequencies (f_{NUM}) to the corresponding dominant values (f_{REC}) of the strongest aftershock (030 in Table 1), the best agreement was found for a bedrock depth of 300 m (Figure 6), value later confirmed by the geophysical surveys, as above mentioned.

Thereafter, two-dimensional time domain SSR analyses were run by the finite elements code QUAD4M (Hudson et al., 1994) with reference to the different geological hypotheses of syncline ('basin' model) and overthrust ('wedge' model) considered in the NNW-SSE direction (Fig. 3).

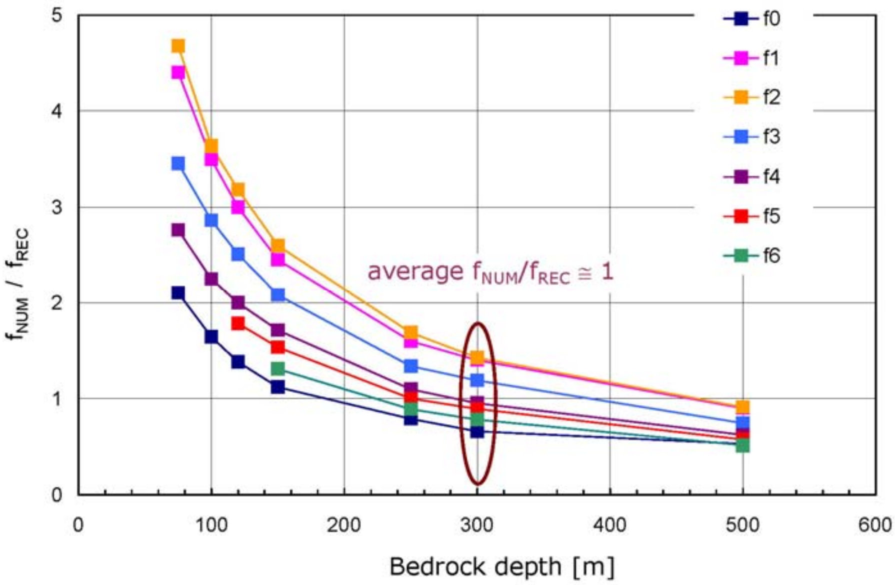

Figure 6. Dependency of the ratio between computed and experimental frequencies on the bedrock depth (after Silvestri et al., 2006b).

For each of the two bedrock geometries considered, five layering patterns corresponding to different degrees of soil heterogeneity were taken into account. All of them are resumed in Table 2, where the letters O and H respectively indicate a homogeneous or heterogeneous formation with respect to the physical and mechanical properties (unit weight, shear and compression wave velocities, Poisson's ratio and initial damping) relevant for the SSR analysis.

Table 2. Models for 2D finite element numerical analyses

Acronym	OO	OOO	HOO	HHO	HHH
Debris cover Tawny clay	homogeneous O	O	heterogeneous H	H	H
Grey clay		O	O	H	H
Faeto flysch	O	O	O	O	H
	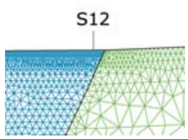	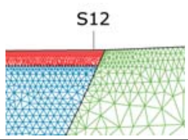	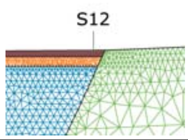	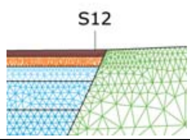	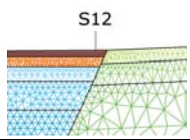
Seismic input	recorded (C_NNW)				de-convoluted (C_NNW_D)

Specific values of the properties adopted are listed in Table 3 for stratigraphic models OO, OOO and HOO; in the first, the clay formation is considered as a whole, while in the second an unique surface cover 7.3m thick is considered, and in the third the two shallow layers (debris and tawny clay) are differentiated. The HHO model assumes for the marly clay unit a variation of velocities with depth following the power law in Fig.4; the pattern defined as HHH, described in detail in Table 4 and Figure 7, presents the maximum degree of heterogeneity, since both the Toppo Capuana formation and the Faeto flysch are assumed to have properties varying with depth.

The drawbacks of the QUAD4M code deriving from wave reflections on the boundaries were prevented by increasing the horizontal and vertical extension of the flysch formation, shown in Fig.7. The transmitting base option was used for the lower boundary, by assigning to the underlying half-space ('bedrock' in Table 4) the same properties as the flysch; the nodes at the lateral boundaries were set as free in the horizontal direction.

Table 3. Properties for OO, OOO and HOO subsoil models

		Debris cover	Tawny clay	Grey clay	Flysch
H [m]		2.4	4.9	variable	variable
γ [kN/m³]	OO	21.20			22.00
	OOO	20.64		21.20	
	HOO	19.60	21.15		
V_S [m/s]	OO	440			1350
	OOO	208		440	
	HOO	122	250		
ν	OO	0.477			0.392
	OOO	0.490		0.477	
	HOO	0.493	0.489		
V_P [m/s]	OO	2100			3200
	OOO	1510		2100	
	HOO	1010	1700		
D_0 [%]	OO	2.5			0.5
	OOO	2.5		2.5	
	HOO	3.0	2.3		

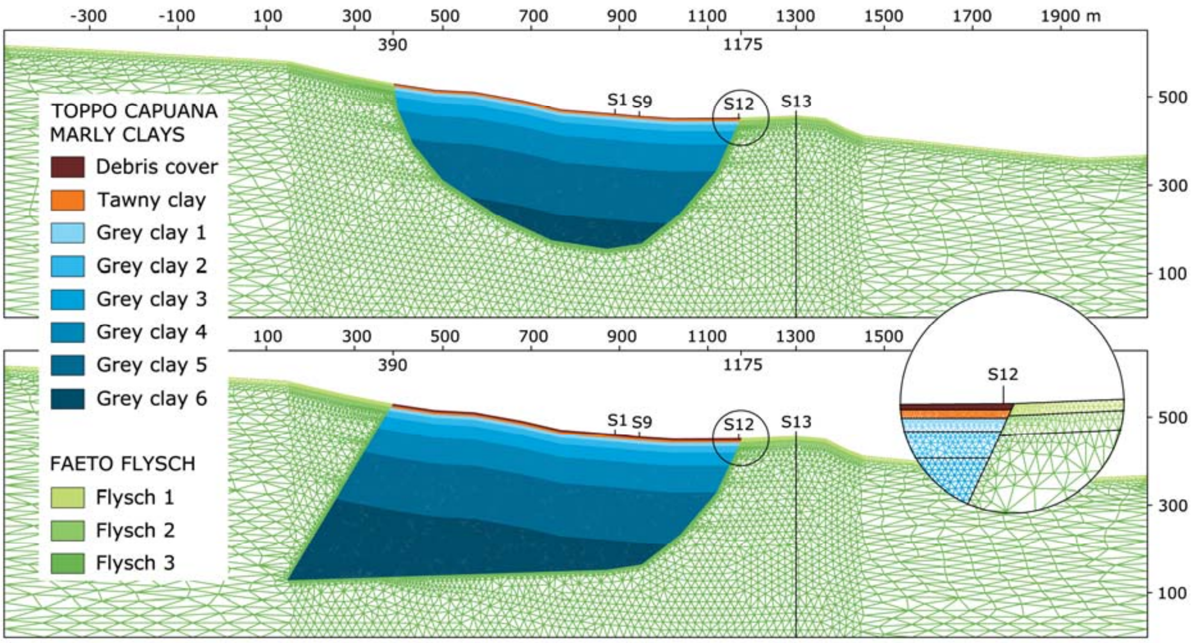

Figure 7. The most heterogeneous (HHH) layering models

Table 4. Properties for heterogeneous subsoil models

	Depth, z [m]	H [m]	γ [kN/m³]	V_S [m/s]	D_0 [%]	ν	V_P [m/s]	h_{MAX} [m]
Debris cover	0 - 2.4	2.4	19.6	122	3	0.493	1010	1.2
Tawny clay	2.4 - 7.3	4.9	21.15	250	2.3	0.489	1700	2.5
Grey clay 1	7.3 - 15	7.7	21.2	339	2.5	0.485	1970	3.4
Grey clay 2	15 - 30	15		364		0.483	2000	3.6
Grey clay 3	30 - 60	30		391		0.481	2050	3.9
Grey clay 4	60 - 120	60		421		0.479	2100	4.2
Grey clay 5	120 - 240	120		454		0.477	2160	4.5
Grey clay 6	> 240	-		483		0.475	2210	4.8
Flysch 1	0 - 6.0	6	22	400	0.5	0.456	1400	4.0
Flysch 2	6.0 - 17.0	11		800		0.443	2500	8.0
Flysch 3	> 17.0	-		1350		0.392	3200	13.5 - 19
Bedrock	-	-	22	1350	0.5	0.392	3200	-

The input motions adopted for the 2D numerical analyses were the horizontal and vertical components of the aftershocks 030 (Nov. 12 am, M_W=4.2) and 040 (Dec. 2 pm, M_L=4.0), as logged by the Church station located close to the S13 vertical, where the Faeto flysch outcrops (Figs. 2,3,7). Due to the high extension and number of elements of the mesh, all the components of the aftershock records were 12.5 Hz low-pass filtered; thereafter, the horizontal components were projected to obtain in-plane motion relative to the section in hand.

Such input accelerograms were used for all the patterns except for HHH. In this latter case, a de-convolution of the signals along the S13 vertical, modelled as a heterogeneous flysch formation (see Table 4 and Fig. 7), was carried out by 1D linear analysis; as a result, the input signals at outcropping bedrock of the HHH model were obtained. The input signals are indicated as C_NNW and C_NNW_D for the recorded and de-convolved accelerograms respectively (Table 2). Analogously, the aftershock recordings at the School station, projected along the NNW-SSE section, are labelled as S_NNW.

In Figure 8 the Fourier spectra of the reference input signals are shown, before and after de-convolution. In the Nov. 12 am record (030C_NNW), the dominant motion frequencies lay approximately around 1.5, 3 and 5.5 Hz. In the Dec. 2 pm record (040C_NNW), with lower magnitude, most of the energy develops around higher frequencies, with the main peaks at 2 and 6 Hz. The de-convolved motions are characterised by the same spectral shape, but the amplitude at the higher frequencies are progressively reduced. The vertical components were applied without any de-convolution procedure.

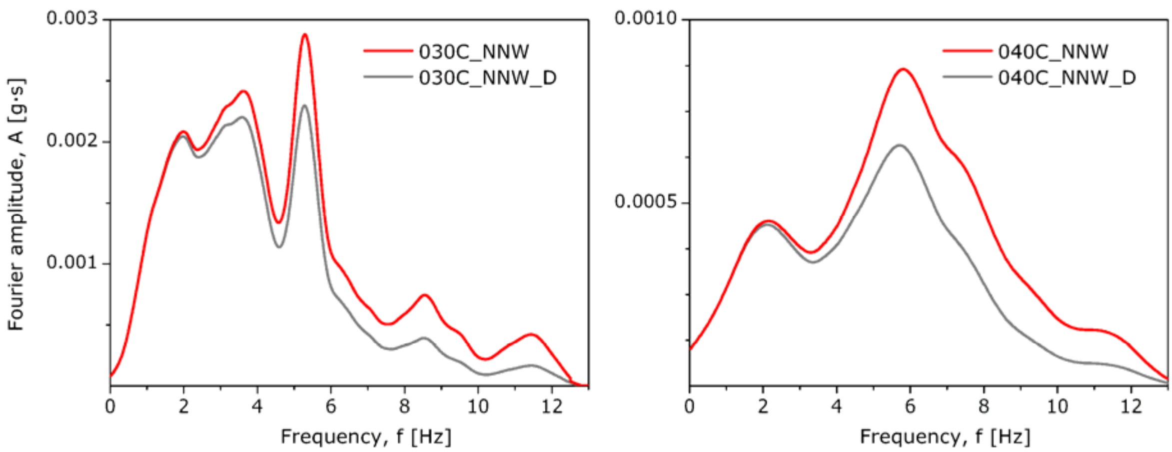

Figure 8. Fourier spectra of input accelerograms

The maximum height of mesh elements, h_{MAX}, for all the materials considered (see Table 4) was fixed according to the well-known condition by Lysmer & Kuhlemeyer (1969):

$$h_{MAX} = \frac{V_S}{8 f_{MAX}} = \frac{V_S}{100} \quad (2)$$

being f_{MAX} equal to 12.5 Hz, i.e. the upper frequency of the low-pass filter applied to the seismic input. The aspect ratio of the elements (i.e. the width divided by the thickness) was set not greater than 3.

RESULTS OF NUMERICAL SIMULATIONS

The distribution of peak horizontal acceleration (PGA) computed along the surface of the NNW-SSE section is shown in Figure 8, for the two adopted geometrical models (basin and wedge) and their associated spatial variation in mechanical properties, as listed in Table 2 and 4; only the results for the highest magnitude seismic event (030) are illustrated. In the same figure, the PGA values recorded at the Church and School stations are also shown.

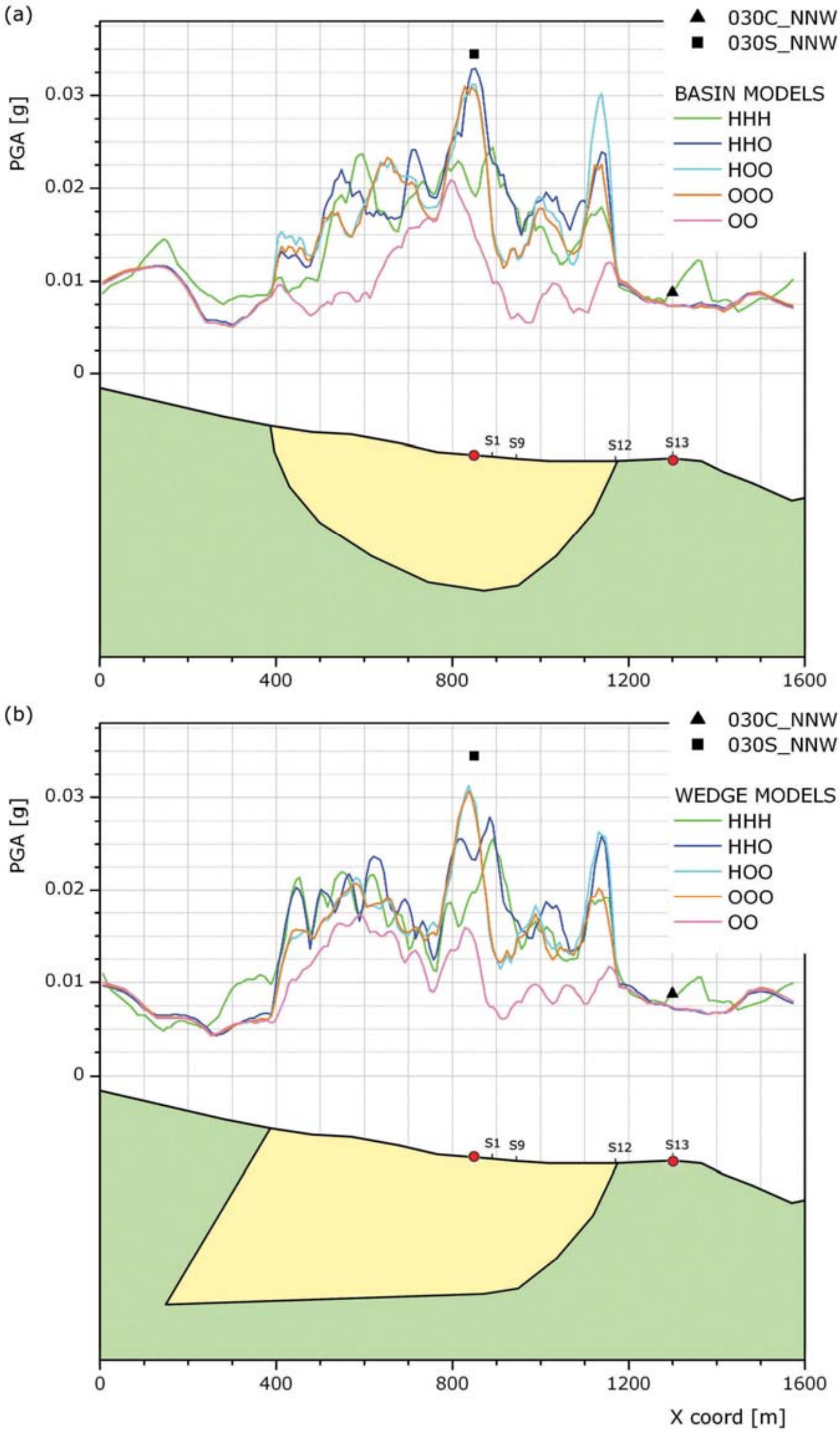

Figure 8. Surface PGA distributions for (a) basin and (b) wedge models

For both basin and wedge models, the peak accelerations along the clay surface result higher than those computed where the flysch outcrops. The computed PGA distributions can be interpreted as a result of complex interaction phenomena between direct P and SV waves and locally generated Rayleigh waves.

On the average, PGA becomes higher moving from the edges toward the center of the clay deposit; nevertheless, a clear fluctuation of the ground motion can be observed, with an average wavelength of about 150m. Such oscillations appear about regular for the basin model, less uniform for the wedge pattern, especially towards the northern flysch-clay contact, where they appear more frequent. This may suggest a likely influence of the deep asymmetric diffraction due to the particular bedrock geometry. Actually, a sequence of zones characterised by different ground motion amplification might be inferred by the irregular damage distribution, found after the mainshock in the recent part of the town lying on the clayey formations (Baranello et al., 2003).

For all the patterns which assume a layered clay deposit, the horizontal ground acceleration abruptly increases at the interfaces between the flysch and clay formations, apparently due to the high impedance ratio among nearby materials. Such effect is not so evident for the HHH model, in which the clay/flysch impedance contrast at surface is less pronounced, and even less appreciable for the OO model, which also shows the lowest estimate of the peak ground acceleration recorded at the School station.

Figure 9 shows the comparison between the experimental and numerical Fourier spectra for the aftershock 030 at the school and church sites, for the basin (left) and wedge (right) configurations. All the Fourier spectra were smoothed with a moving Hanning window of width 1.2 Hz.

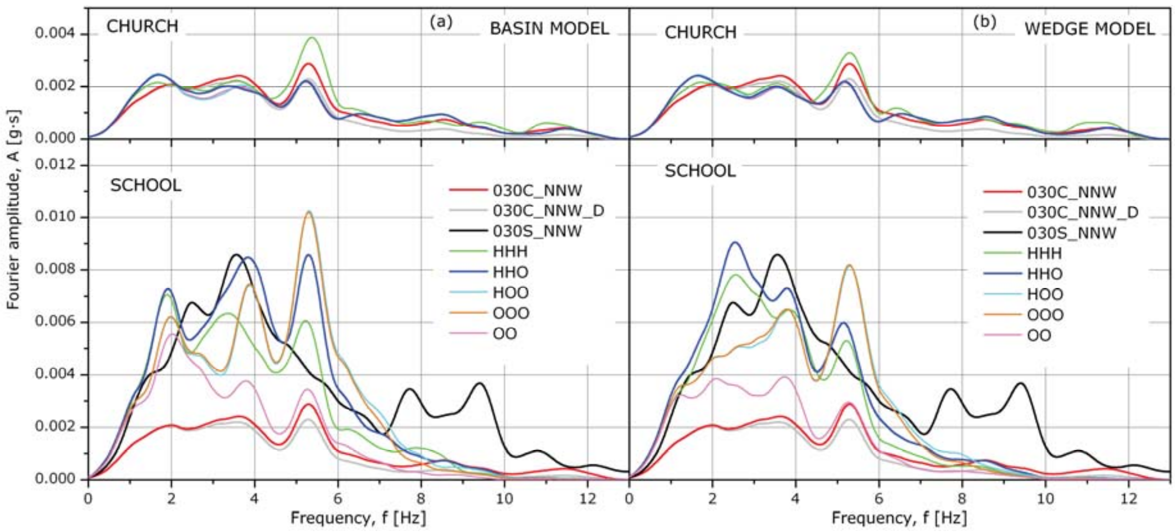

Figure 9. Comparison between recorded and simulated Fourier spectra for basin and wedge models at church and school sites: (a) aftershock 030 (M_W=4.2); (b) aftershock 040 (M_L=4.0)

It can be noted that the Fourier spectrum recorded at the church site (red line) is generally well reproduced by the numerical analyses, for both morphological configurations.

With reference to the school site, all models show a satisfactory agreement with the experimental results for frequencies lower than 2 Hz. For both basin and wedge configurations, the Fourier spectra relevant to the HHO and HHH models appear close to the record in the range 2-7 Hz. In the basin structure, the HHO pattern reproduces the experimental peaks at 3.5 Hz better than HHH. In the wedge configuration, the numerical prominent peak for both layering patterns is about 1 Hz shifted towards frequencies lower than the experimental; the amplitude of the computed spectrum is, however, very close to the measured one. It is worth observing that all models present a peak at around 5 Hz not shown by recordings; they also fail in reproducing the experimental spectral density for frequencies higher than 7 Hz. This unconsistency might be due to either 3D subsoil geometry (as recently confirmed by the gravimetric profiling by Palmieri et al., 2006) and/or propagation of spurious short waves, for instance scattered by buildings along surface; such effect cannot of course be reproduced by free-field seismic response models.

Simple parameters were introduced to obtain an objective synthetic estimate of the matching between experimental and numerical results, both in time and frequency domain. In time domain, the ratio between predicted and recorded PGA was considered: a good agreement between experimental results and numerical predictions is obviously characterised by an acceleration ratio very close to unity. In the frequency domain, the spectral matching was quantified by the root-mean-square deviation of the numerical spectrum from the experimental one, computed in the frequency range 1-12.5 Hz:

$$\sigma = \sqrt{\frac{1}{N}\sum_{i=1}^{N}\left(A_{i,NUM} - A_{i,REC}\right)^2} \tag{3}$$

where N is the number of frequency values at which the spectral shape is specified, $A_{i,NUM}$ is the spectral amplitude at frequency f_i computed from the numerical analysis, $A_{i,REC}$ is the value at the same frequency obtained from the recordings. The smaller the value of σ, the closer the match between the shape of the recorded spectrum and that numerically simulated.

Table 5 shows the summary of the σ values computed at the School and Church sites, for the most reliable hypotheses (HOO, HHO, HHH) on the layering of both geological models. On the whole, the peak amplitudes recorded at the School site are systematically underestimated by the simulations of the event 030, and most times overestimated for the other aftershock. The HOO hypothesis provides the worst approximation of the frequency content for both seismic records considered. The wedge configuration shows the better agreement with the experimental frequency content but yields a worse estimate of recorded PGA.

Table 5. Synthetic compatibility parameters

		σ [g·s]		PGA_{NUM}/PGA_{REC}			
		Church + School values		Church	School	Church	School
		030	040	030		040	
Basin	HHH	0.00184	0.00056	1.015	0.557	1.5315	1.0649
	HHO	0.00185	0.00062	0.838	0.957	0.8760	1.3484
	HOO	0.00234	0.00106	0.829	0.906	0.8760	1.7461
Wedge	HHH	0.00174	0.00056	0.977	0.579	1.5193	0.7856
	HHO	0.00177	0.00046	0.831	0.671	0.8525	0.8926
	HOO	0.00198	0.00061	0.840	0.870	0.8343	1.1726

CONCLUSIONS AND PERSPECTIVES

The paper describes the subsoil models set up for analyzing the site amplification that significantly affected the non-uniform distribution of building damage in the town of San Giuliano di Puglia, due to the Molise earthquake sequence, started on October 31, 2002.

The comprehensive geotechnical investigation carried out soon after the earthquake for the seismic microzonation of the town has been briefly described in the paper. The merge between field and laboratory experimental data allowed a detailed definition of the subsoil model at relatively high depths. The results of geophysical tomographies and the analysis of frequency content of the aftershocks indicated a thickness of about 300 m for the marly clay formation beneath the recent part of the town. However, a full description of the bedrock geometry is expected to be achieved from the execution of a forecoming deep seismic reflection survey.

In the meantime, to envisage a more reliable definition of the subsoil model, 2D seismic response analyses were carried out by QUAD4M on a section developing along the longitudinal axis of the town. Two different bedrock geometries were assumed, i.e. a 'basin' and a 'wedge' shape, respectively referring to a syncline and an overthrust geological model. For each configuration, five different spatial distributions of soil properties were compared. The assessment of the numerical predictions was obtained comparing the computed ground accelerations with the values recorded during two aftershocks, in terms of horizontal peak values and frequency contents.

Although the large scale geophysical tests showed an apparent 3D subsoil structure, the 2D analyses were able to reproduce both qualitatively and quantitatively the measured ground motion. In particular, the better response shown by the heterogeneous layering models highlighted the influence of the stratigraphic details on the seismic motion at surface.
Furthermore, the analyses provided a PGA distribution along the ground surface increasing from the edges to the center of the clay deposit, and characterised by longitudinal fluctuations. This result is consistent with the irregular seismic damage distribution observed in the recent part of the town. The syncline basin configuration showed a better prediction of ground motion amplitudes, while the hypothesis of an overthrust wedge structure appears more accurate in predicting the frequency content.

At present, further numerical analyses on a large scale 3D model are in progress, care of the INOGS (Trieste), in the framework of the INGV-S3 Project. The use of both 2D and 3D models are expected to provide the support for reliable simulations of the damage scenario during the main event of October 31, 2002.

ACKNOWLEDGMENTS

The work is part of the *INGV-S3 Research Project*, promoted by *National Institute of Geophysics and Vulcanology* (INGV) and funded by the *Department of Civil Protection* (DPC) of the Italian Government. The authors wish to thank the DPC and the project team coordinators, Dr. Francesca Pacor and Prof. M. Mucciarelli, for their valuable scientific and administrative support. All the people previously contributing to the subsoil characterisation and the preliminary seismic response analyses (F. Cotecchia, A. d’Onofrio, A. Guerricchio, C. Petillo, F. Santucci de Magistris, C. Vitone) are also warmly acknowledged.

REFERENCES

Baranello S., Bernabini M., Dolce M., Pappone G., Rosskopf C., Sanò T., Cara P.L., De Nardis R., Di Pasquale G., Goretti A., Gorini A., Lembo P., Marcucci S., Marsan P., Martini M.G. and Naso G., “Rapporto finale sulla Microzonazione Sismica del centro abitato di San Giuliano di Puglia”. Dipartimento di Protezione Civile, Roma, 2003 (in Italian).

Guerricchio A., Personal communication, 2005.

Hudson M., Idriss I. M. and Beikae M., “Quad4M-A computer program to evaluate the seismic response of soil structures using finite element procedures and incorporating a compliant base”, University of California, Davis, California, 1994.

Lysmer J. and Kuhlemeyer L. “Finite dynamic model for infinite media”, Journal of the Engineering Mechanics Division, pp. 859-877, 1969.

Melidoro G., Personal communication, 2004.

Mucciarelli M., Masi A., Vona M., Gallipoli M. R., Harabaglia P., Caputo R., Piscitelli S., Rizzo E., Picozzi M., Albarello D. and Lizza C., “Quick survey of the possible causes of damage enhancement observed in San Giuliano after the 2002 Molise, Italy seismic sequence”, Imperial College Press, Journal of Earthquake Engineering, 7, Issues 4, 599–614, 2003.

Palmieri F., Marello L. and Priolo E., “Rilievo gravimetrico di dettaglio nell’area di San Giuliano di Puglia (CB)”, INOGS Research Report, S3 Project, 2006 (in italian).

Ranieri N., Clemente P., Renzi E. and De Canio G., “Indagini diagnostiche su un edificio scolastico a seguito del terremoto del Molise”, Act of XI National Conference “L’ingegneria Sismica in Italia”, Genova (Italy), January 25-29, 2004 (in Italian).

Petillo C., “Risposta sismica del centro abitato di San Giuliano di Puglia”, Master's Degree Thesis in Geotechnical Engineering, University of Napoli “Federico II”, 2004 (in Italian).

Puglia R., “Analisi della risposta sismica locale di San Giuliano di Puglia”, Research report, University of Calabria, 2005 (in Italian).

Silvestri F., Vitone C., d’Onofrio A., Cotecchia F., Puglia R. and Santucci de Magistris F., “The influence of meso-structure on the mechanical behaviour of a marly clay from low to high strains”, Symposium to celebrate Prof. Tatsuoka's 60th birthday, Roma (Italy), 2006a.

Silvestri F., d’Onofrio A., Guerricchio A., Lanzo G., Pagliaroli A., Puglia R., Santucci de Magistris F., Sica S., Eva C., Ferretti G. and Di Capua G., “Modelli geotecnici 1D e/o 2D per i comuni di San Giuliano di Puglia, Bonefro, Ripabottoni, Colletorto e Santa Croce di Magliano”, Deliverable D8, S3 Project. internet: http://esse3.mi.ingv.it/S3_doc.html, 2006b (in Italian).